

Study of ^{14}Be with core excitation

T. Tarutina ^{a,b,1}, I.J. Thompson ^a, J.A. Tostevin ^a

^a*Department of Physics, University of Surrey, Guildford GU2 7XH, U.K.*

^b*Departamento de Física Nuclear, Instituto de Física da Universidade de São Paulo, Caixa Postal 66318, 05315-970 São Paulo, Brazil*

Abstract

The heavy beryllium isotopes ^{13}Be and ^{14}Be are described as one- and two-neutrons outside of a deformed ^{12}Be core, which is treated as a rigid rotor and the neutron-core interaction is approximated by a deformed Woods-Saxon potential. Our three-body description of ^{14}Be uses the hyperspherical expansion formalism, including the core degrees of freedom. We explore those potential parameters compatible with the known properties of ^{12}Be , ^{13}Be and ^{14}Be . We find that both ^{14}Be and ^{13}Be can be described simultaneously provided the ^{12}Be core has a large positive quadrupole deformation.

PACS numbers: 21.60.-n, 21.10.-k

Key words: ^{13}Be ; ^{14}Be ; particle-rotor model with core excitation; hyperspherical harmonics method;

1 Introduction

The ^{14}Be nucleus is a good candidate for having a neutron halo structure and both ^{14}Be and its subsystem ^{13}Be have been the subject of several recent experiments and theoretical calculations. In this work we perform a simultaneous study of the properties of both ^{13}Be and ^{14}Be , described as few-body systems with a ^{12}Be core and one- or two-neutrons. The ^{12}Be core is assumed rotational and is allowed to excite to its first 2^+ state. These few-body structure models rely on a knowledge of the underlying potentials between the constituents and hence on the structures of each of the underlying two-body subsystems. To understand ^{14}Be one must at the same time understand ^{13}Be .

¹ Electronic address: tatiana@fma.if.usp.br

The known experimental information on the ^{14}Be , ^{13}Be and ^{12}Be nuclei is outlined below and the results of some earlier theoretical descriptions are discussed. The two-neutron separation energy of ^{14}Be has been the subject of two experiments. The first, a pion double charge-exchange measurement [1], gave 1.12 ± 0.16 MeV. The second, time-of-flight experiment [2], gave 1.48 ± 0.14 MeV. The usually cited value, $S_{2n} = 1.34 \pm 0.11$ MeV [3], is the weighted average of these. An experiment by Labiche *et al.* [4] studied the dissociation of ^{14}Be at 35 MeV/nucleon on carbon and lead targets in a kinematically complete measurement. Comparisons of the data with three-body model calculations suggested that the ground state wave function of ^{14}Be includes a strong $[2s_{1/2}]^2$ state admixture.

There have been a series of experiments to study ^{13}Be [5–8]. That ^{13}Be is unbound was suggested more than 30 years ago [9,10], and confirmed in 1973 [11]. Although the detailed results and conclusions drawn from the available experiments are quite different, they do all agree that ^{13}Be has an excited state at approximately 2.0 MeV with spin-parity $\frac{5}{2}^+$. Recently Thoennessen *et al.* [12] found the first evidence for low-lying s -wave strength in ^{13}Be . Those authors show that the experimental data are consistent with simulations if one assumes the ground state of ^{13}Be is an s -state with a scattering length $a_s < -10$ fm, and which corresponds to a virtual state at relative energy less than 200 keV.

The nucleus ^{12}Be has also been studied [13,14] using the $^{10}\text{Be}(t,p)^{12}\text{Be}$ reaction. Fortune *et al.* [14] reported five low-lying states of ^{12}Be with $E_x = 0.0(0^+)$, $2.1(2^+)$, $2.7(0^+)$, $4.6(2^+)$ and $5.7(4^+)$ MeV, where the spin assignments of the last three states are only tentative. In recent years much evidence has been accumulated that ^{12}Be does not have a good $N = 8$ neutron closed shell [15–17]. Iwasaki *et al.* [15] observed a strong excitation of the ^{12}Be 2_1^+ state in inelastic proton scattering from ^{12}Be , consistent with a strong quadrupole deformation. The associated coupled-channels analysis deduced a deformation length $\delta=2.00\pm 0.23$ fm for this state (corresponding to $\beta = 0.728\pm 0.084$ when $R = 1.2 \times A^{1/3}$), confirming that the closed shell structure does not prevail in ^{12}Be . The most direct observation of the disappearance of the $N = 8$ closed shell in ^{12}Be arises from the one-neutron knockout reaction, measured at MSU on a ^9Be target [16]. The spectroscopic factors and momentum distributions of the ^{11}Be residues in their $1/2^+$ ground state and $1/2^-$ excited state reveal that the last neutrons have a significant $[2s_{1/2}]^2 + [1d_{5/2}]^2$ configuration and that there is only of order 30% of the $[1p_{1/2}]^2$ closed shell component.

There have also been several theoretical analyses of the structure of ^{13}Be and ^{14}Be . Most of these assume that ^{13}Be has a $1d_{5/2}$ resonance at 2 MeV and has a low-lying spin $1/2$ state – a p -wave resonance or a s -wave virtual state. Bertsch and Esbensen investigated ^{13}Be and ^{14}Be using a two-neutron pairing model [18] in which ^{14}Be is described as an inert core and two interacting

neutrons. The ^{14}Be two-neutron separation energy, $S_{2n} = 1.34 \pm 0.11$ MeV, was reproduced for a ^{13}Be $d_{5/2}$ resonance at 2.4 MeV and an unbound $2s_{1/2}$ ground state. A similar model was employed in the work by Labiche *et al.* [19], which proposed several different scenarios for the structure of $^{13,14}\text{Be}$, fixing the $d_{5/2}$ resonance at 2 MeV. Their model however predicts a $1/2^-$ ground state in ^{13}Be . The Faddeev three-body approach was used by Thompson and Zhukov [20], also treating ^{14}Be as an inert ^{12}Be core interacting with valence nucleons via a single channel ℓ -dependent Woods-Saxon potential. It was found that in order to keep ^{13}Be unbound, and at the same time to describe correctly the binding of ^{14}Be , the position of the $d_{5/2}$ resonance had to be lowered to 1.3 or 1.0 MeV. In contrast to the macroscopic calculations described above, a microscopic three-cluster model was used by Descouvemont [21]. These calculations required that the s -wave ground state in ^{13}Be is slightly bound, with an energy -19 keV, and the $d_{5/2}$ resonance is at the measured energy, 2 MeV. The calculations showed an increased rms radius compared to that of ^{12}Be and a comparatively large excited core component in the total wave function. The microscopic ^{12}Be -neutron potential derived by Descouvemont was used in Lagrange-mesh calculations of ^{14}Be by Adahchour *et al.* [22], and later more accurately by Baye [23]. The Lagrange-mesh techniques have proved to give a simple and accurate solution of the three-cluster $^{12}\text{Be}+n+n$ Schrödinger equation. The calculations show that a renormalisation of the core-neutron potential, by a factor 1.06, is needed in order to generate a separation energy of ^{14}Be of 1.18 MeV.

The above overview shows that a simultaneous description of the ^{14}Be Borromean system and its unbound daughter ^{13}Be is not an easy task. To describe correctly the binding of ^{14}Be one has to assume either a bound s -wave ground state of ^{13}Be or an unbound ^{13}Be , but with a p -wave ground state. Neither scenario is consistent with the experimental data.

In this work an excited core model [24–26] is used to attempt to describe ^{13}Be and ^{14}Be as one- or two-neutrons outside of a deformed ^{12}Be core. The previous inclusion of such core excitation, of ^{10}Be , made it possible to describe ^{11}Be as a $2s$ -intruder state nucleus. The approach was also used by Esbensen *et al.* [27] to describe positive parity states of ^{11}Be and by Ridikas *et al.* [28] to study a series of carbon isotopes.

The basic idea of the method is that the deformation of the core leads to couplings with core excited configurations. For the two-body structure we assume a particle-rotor model. The advantage of this approach is that the inclusion of core degrees of freedom is physically transparent and simplifies the calculations. To solve the three-body ^{14}Be problem, the hyperspherical expansion method is used. This method is widely used nowadays to describe the characteristics of light exotic nuclei. The advantage of this method is that it uses an expansion over a complete set of orthonormal functions, which re-

duces the three-body problem to a set of one-dimensional hyperradial coupled equations whose solution is translationally and rotationally invariant. Another important advantage of this method, for Borromean nuclei, is that the correct three-body asymptotic behavior is assured. A known disadvantage is the relatively slow convergence of the three-body energy eigenvalues with the number of hyperspherical harmonics used.

This paper is organized as follows. In Section 2 we describe briefly the two-body and three-body models used for the structure calculations of ^{13}Be and ^{14}Be . In Section 3 we explore those potential parameters which are compatible with the known properties of ^{12}Be , ^{13}Be and ^{14}Be . Finally, Section 4 contains a summary and conclusions.

2 Theoretical background

2.1 Two-body model

The total Hamiltonian \hat{H} of the core plus neutron two-body system can be written

$$\hat{H} = \hat{T}_r + \hat{h}_c(\vec{\xi}) + \hat{V}_{nc}(\vec{r}, \vec{\xi}), \quad (1)$$

where \hat{T}_r is the kinetic energy of the relative motion of the core and valence neutron, $\hat{h}_c(\vec{\xi})$ is the core Hamiltonian, which depends on the internal variables $\vec{\xi}$, and $\hat{V}_{nc}(\vec{r}, \vec{\xi})$ is the interaction between the core and the neutron. The total wave function of the system, with total angular momentum J and projection M , is expanded in terms of the core states ϕ_I as

$$\Psi_{JM}^{(2)} = \sum_{l,j,I} \frac{\chi_{ljI}^J(r)}{r} \{[Y_l \otimes X_s]^j \otimes \phi_I\}^{JM}, \quad (2)$$

where the Y_l are spherical harmonics and the X_s are spin functions. The rotational model is assumed for the structure of the core, hence the core is a deformed axially symmetric rotor and the ϕ_I are proportional to rotation matrices. In the body-fixed frame the radius of this deformed core is expanded in spherical harmonics and, for simplicity, we retain only the quadrupole term, as

$$R(\theta', \phi') = R_0 \left[1 + \beta Y_{20}(\theta', \phi') \right]. \quad (3)$$

For the core-neutron interaction, we assume a deformed Woods-Saxon potential but with an undeformed spin-orbit term,

$$V_{nc}(r, \theta', \phi') = \frac{V_0}{1 + e^{\frac{r-R(\theta', \phi')}{a}}} - 2\left(\frac{\hbar^2}{m_{\pi}c}\right)^2 \frac{V_{ls}}{r} \frac{d}{dr} \frac{1}{1 + e^{\frac{r-R_{ws}}{a_{ws}}}} \mathbf{l} \cdot \mathbf{s}. \quad (4)$$

The same deformation parameter is assumed for all core states.

2.2 Three-body model

The three-body Hamiltonian of the system, after separation of the center of mass motion, is written

$$\hat{H} = \hat{T}_x + \hat{T}_y + \hat{h}_c(\vec{\xi}) + \hat{V}_{nc}(\mathbf{r}_{1C}, \vec{\xi}) + \hat{V}_{nc}(\mathbf{r}_{2C}, \vec{\xi}) + \hat{V}_{nn}(\mathbf{x}, s_x, l_x), \quad (5)$$

where \hat{T}_x and \hat{T}_y are the kinetic energy operators associated with the normalized Jacobi coordinates $x = \sqrt{\frac{A_1 A_2}{A_1 + A_2}} X$ and $y = \sqrt{\frac{(A_1 + A_2) A_C}{A_1 + A_2 + A_C}} Y$ (see Fig. 1). Here \vec{r}_{1C} and \vec{r}_{2C} are the vectors connecting neutron 1 and neutron 2 with the core and, as previously, \hat{h}_c is the core Hamiltonian and $\vec{\xi}$ represents the internal coordinates (Euler angles) of the core. In the \mathbf{T} -coordinate system the total wave function is expanded in terms of the core wave functions. Let J and M be a total angular momentum and its projection, l_x and l_y be the orbital angular momenta in the x and y coordinates and I be a spin of the core, then

$$\Psi_{JM}^{(3)} = \sum_{l_x l_y L S I j} \psi_{l_x l_y}^{LSjIJ}(x, y) \left\{ ([Y_{l_x} \otimes Y_{l_y}]^L \otimes [X_{s_1} \otimes X_{s_2}]^S)^j \otimes \phi_I \right\}^{JM}. \quad (6)$$

The radial wave functions, which depend on $x = |\mathbf{x}|$ and $y = |\mathbf{y}|$, are expanded in the hyperspherical harmonics which are defined using the hyperspherical variables ρ and α ,

$$\rho = \sqrt{x^2 + y^2}, \quad \alpha = \arctan\left(\frac{x}{y}\right). \quad (7)$$

The hyperspherical expansion of the three-body radial wave function is

$$\begin{aligned} \psi_{l_x l_y}^{LSjIJ}(x, y) &= \rho^{-\frac{5}{2}} \sum_K \chi_{K l_x l_y}^{LSjIJ}(\rho) \phi_K^{l_x l_y}(\alpha), \\ \phi_K^{l_x l_y}(\alpha) &= N_K^{l_x l_y} (\sin \alpha)^{l_x} (\cos \alpha)^{l_y} P_n^{l_x + \frac{1}{2}, l_y + \frac{1}{2}}(\cos 2\alpha), \end{aligned} \quad (8)$$

where $P_n^{l_x+\frac{1}{2}, l_y+\frac{1}{2}}(\cos 2\alpha)$ is the Jacobi polynomial and $N_K^{l_x l_y}$ is a normalization coefficient. K is the hyperangular momentum quantum number $K = l_x + l_y + 2n$ ($n = 0, 1, 2, \dots$). Full details of the formalism of the hyperspherical harmonics method, when including core excitation, is presented in Refs. [30,25].

As for the two-body system, for the core-neutron interaction we use a deformed Woods-Saxon potential and spherical spin-orbit term, defined in Eq. (4). The neutron-neutron (NN) interaction was approximated by the GPT local potential [29]. We used the simplified version of the GPT potential and neglected the quadratic spin-orbit term in the NN interaction.

2.3 The Pauli Principle

In the two-body case, without core excitation, the Pauli principle is included automatically, if it is assumed that the core neutrons occupy low-lying states defined by the core-neutron interaction. The core states are then automatically orthogonal to any valence states.

In the three-body case the wave function of the system should be antisymmetrized with respect to (a) the permutation of the two halo nucleons, and (b) exchange of neutrons between the core and halo. The first requirement is easily satisfied by imposing the appropriate selection rule in the \mathbf{T} coordinate system. To satisfy the second, the wave function should be antisymmetric with respect to the permutation of a halo and a core neutron. This part of the Pauli principle is treated in an approximate way by requiring that the three-body wave function of the system is orthogonal to the occupied core plus neutron states, taken as the low-lying eigenstates of the deformed-core and neutron two-body Hamiltonian. Once these states are constructed, the projection operator on to the forbidden states space can be defined and they can be projected out of the allowed three-body space, according to the standard Feshbach procedure [32,33]. Details can be found in [30]. Such an approach is well suited to the treatment of core nuclei with closed shells.

In using this approximation in the present study we assume that ^{12}Be is a closed p -shell nucleus, although, as discussed above, this is not the case. If ^{12}Be is assumed spherical and inert the $1s_{1/2}$, $1p_{1/2}$, and $1p_{3/2}$ states are occupied. When core excitation is included, instead of these three states we have 11 blocked eigenstates coupled with the ground and excited states of the core.

3 Results of two- and three-body calculations

Using the particle-rotor model described above, we now explore the parameters (V_0, β, V_{ls}) of the two-body core-neutron potentials to see which, if any, are compatible with the available experimental data. Our aim, in the case of ^{13}Be , is to find parameter values which position the $5/2^+$ resonance at 2 MeV and simultaneously place a $1/2^+$ state near to threshold.

3.1 Deformed core calculations for ^{13}Be

We study the properties of ^{13}Be calculated upon variation of the core deformation β , the spin-orbit potential depth V_{ls} and the central Woods-Saxon potential depth V_0 . To calculate the positions of the $5/2^+$ resonances and the energies of the bound or virtual $1/2^+$ states we used the R-matrix method on a Lagrange mesh (see [31], and references therein), which allows bound and continuum states to be found from the same small basis set. The energies of the $\frac{1}{2}^+$ virtual states are determined using second-order effective range theory. The criterion for a $\frac{5}{2}^+$ resonance at certain energy is that the phase shift is equal to $\pi/2$ at this energy.

We assume throughout a standard Woods Saxon geometry, with radius $r_0 = 1.2$ fm ($R_0 = r_0 A^{1/3}$) and diffuseness $a = 0.65$ fm. The same parameters are assumed in the spin-orbit potential. Although the ^{12}Be deformation has been estimated as $|\beta| = 0.728 \pm 0.084$ [15], we carry out calculations for the full range of the deformation parameter $\beta \in [-1 : 1]$.

The ^{13}Be system has the interesting feature that the observed $5/2^+$ resonance energy at 2 MeV is very close to the excitation energy of the ^{12}Be 2^+ state of 2.1 MeV. Hence, it is natural to suggest that the existence of a $5/2^+$ resonance in ^{13}Be may be connected with the core excitation of ^{12}Be , and that the $5/2^+$ resonance will contain a large amount of $[2s_{1/2} \otimes 2^+]5/2^+$ core excited component. Consequently, we can expect two $5/2^+$ resonances in this system, which, for small values of core deformation, are build on an inert core $[1d_{5/2} \otimes 0^+]5/2^+$ and on the excited core $[2s_{1/2} \otimes 2^+]5/2^+$. For larger core deformation this simple labeling will not work since, due to the strong core state couplings, the admixtures of other components in the wave function, for both resonances, becomes large. In the calculations we adjust parameters so that the lower of the two $5/2^+$ resonances is at 2 MeV because no lower state was seen experimentally.

Obviously, the dependence of the energy of the $1/2^+$ state on the spin-orbit strength is small, since the dependence is only through couplings with the

$[1d_{5/2} \otimes 2^+]1/2^+$ and $[1d_{3/2} \otimes 2^+]1/2^+$ configurations, although that of the $5/2^+$ state changes significantly. We can thus assume that the position of the $1/2^+$ state is governed primarily by V_0 and that of the $5/2^+$ state adjusted using V_{ls} . To obtain a $1/2^+$ state near threshold, and unbound, and the $5/2^+$ state at 2 MeV, we must choose a relatively shallow central potential and a small spin-orbit strength. We note that the simplest mean-field descriptions place the $2s_{1/2}$ state above the $1d_{5/2}$.

To obtain Fig. 2 we fix V_0 and V_{ls} and vary the core deformation β . This graph is similar to a Nilsson plot except that, in the Nilsson model, the projection of total angular momentum on the symmetry axis is used while here we project the angular momentum on to the laboratory z -axis. Since V_0 in this case is the same for all values of deformation, the $5/2^+$ state is not fixed at 2 MeV. The fixed V_0 was chosen here to obtain an unbound ^{13}Be and the $5/2^+$ state at 2 MeV in the case of zero deformation, requiring $V_{ls} = -8$ MeV. It is seen that, with increasing β , the stronger coupling with the excited core lowers the energies of the states. The behavior of the lowest $5/2^+$ state is, in general, consistent with that of the $1d_{5/2}$ curve on a Nilsson plot. The behavior of the $1/2^+$ state is consistent with that observed for the $1/2^+$ state in ^{11}Be [27,24].

There also appears here a second $5/2^+$ resonance, which develops non-zero width for $\beta \neq 0$ by coupling the entrance channel to a $[2s_{1/2} \otimes 2^+]$ configuration when the $2s_{1/2}$ is bound or nearly bound. As the $2s_{1/2}$ state becomes unbound when $\beta \sim 0$, the width of this state becomes vanishingly small. There is an avoided crossing for small β .

We next fix the lowest $5/2^+$ state at 2 MeV and investigate whether ^{13}Be remains unbound in some regions of β . As is seen from the Nilsson graphs, to maintain the $5/2^+$ state at a fixed energy of 2.0 MeV, we need to weaken V_0 with increasing β . These calculations were performed for several values of V_{ls} , from the more usual value of -7 MeV, to -1 MeV. The results for the $1/2^+$ state are presented in Fig. 3. The figure shows that the smaller $|V_{ls}|$, the lower the position of the $1/2^+$ state. This behavior is understood from the following considerations. With a large $|V_{ls}|$ we have to reduce V_0 in order to place the $5/2^+$ resonance at 2 MeV. Conversely, for small $|V_{ls}|$, V_0 must be increased and the position of $1/2^+$ level goes down. For $V_{ls} = -1$ MeV, ^{13}Be is bound for all values of β . When we increase $|V_{ls}|$, ^{13}Be becomes unbound in the regions of large β . This can be understood from the Nilsson-like graph in Fig. 2, where the energies of the $1/2^+$ and $5/2^+$ states fall with deformation and the position of the $5/2^+$ state falls faster than that of the $1/2^+$ state. To compensate for this decrease, and fix the $5/2^+$ state at 2 MeV, we must reduce the V_0 with β . For $|V_{ls}| \approx 2$ MeV and greater, ^{13}Be is unbound for some values of β , and these regions increase with increasing $|V_{ls}|$. For small β , a peculiar behavior of the $1/2^+$ energies can be seen, a consequence of the two $5/2^+$ resonances being very close in energy.

Figure 4 clarifies the structure of the lowest of the $5/2^+$ resonances, fixed at 2 MeV, and shows the percentage of core excited state components in the resonance wave function. For small $|V_{ls}|$ the $5/2^+$ resonance is built on the excited core. With increasing spin-orbit depth, from -5 to -6 MeV, the resonance changes its nature and becomes built on the ground state of the core. For large positive β the $5/2^+$ resonance contains large amounts of both inert core and excited core components and so cannot be attributed to either the inert core or excited core resonance. For large core deformations β , the model predicts ^{13}Be is unbound for a significant range of spin-orbit potentials. We note that in the region of small deformations, for spin-orbit strengths between -6 and -5 MeV the resonance changes nature, as the avoided crossing requires a $5/2^+$ state of different intrinsic structure to be located at $+2.0$ MeV

3.2 Deformed core calculations for ^{14}Be .

The two-body potentials found in the previous Section are now used to calculate the ground state energies of ^{14}Be , described as a three-body system.

The convergence of the three-body energy with the number of hyperspherical harmonics is presented in Fig. 5, and is seen to be rather slow. Given this rate of convergence the Feshbach reduction method was used to reduce the computation time. In the Feshbach reduction, the number of coupled-channels equations solved explicitly is reduced by introducing an additional operator which takes into account, approximately, the remaining channels [34]. Two curves are shown in the figure. The first, the open circles and dashed line, shows the results of the full coupled channels calculations. The second, the open squares and dotted line, shows the results when using the Feshbach reduction method. Calculations were performed to include a maximum number of hyperspherical harmonics $K_{max} = 26$. Those channels up to K_{max} , but with $K > 12$, were treated approximately by the reduction. The two calculation schemes are shown to overlap in the central region of the figure, and the method gives a three-body energy very close to that obtained from the full calculation, but with a much reduced computation time.

The three-body energy of the ground state of ^{14}Be was calculated using many of the sets of two-body potentials obtained in the previous section for V_{ls} from -7 MeV to -1 MeV. Figure 6 shows the three-body separation energies which result.

We observe that the binding of ^{14}Be increases with the deformation as is expected from the general observation that inclusion of core degrees of freedom adds binding to the system.

We discuss below the regions of β and potential parameters which lead to a

consistent, simultaneous description of ^{13}Be and ^{14}Be . As the results of the two measurements of the separation energy of ^{14}Be are quite different (see Section 1), our objective was to obtain a separation energy for ^{14}Be of at least 1 MeV. The calculated three-body energies for different V_{ls} and β are shown in Fig. 6, where we fix V_{ls} and change β so the lowest $5/2^+$ state is at 2 MeV. The three-body energy is not symmetric with respect to the sign of β , which can be understood with reference to the Nilsson graph of the previous Section. For large positive β , coupling with the core excited state adds more binding to the system. For large negative β , coupling reduces the three-body separation energy. For small deformations the behavior of the three-body energy is more complicated, the basis of which is the proximity of two $5/2^+$ resonances in ^{13}Be in this case.

For a fixed β the three-body binding is stronger for smaller spin-orbit depths. This is connected to the fact that, to place the $5/2^+$ state in ^{13}Be at 2 MeV, we have to choose a weaker V_0 in the case of strong V_{ls} . For large β the dependence of the three-body energy on $|V_{ls}|$ is approximately linear. Figure 7 shows that for negative β we have only a small region of parameters where the binding energy of ^{14}Be exceeds 1 MeV, whereas for positive β we have a more extended range of parameters.

The next step is to compare these results with the binding energies in the ^{13}Be subsystem. In the area above the solid curve in Fig. 7 ^{13}Be is unbound. We see that for positive β the two areas overlap and so we have a region of parameters where both ^{13}Be and ^{14}Be are described simultaneously. For negative β the three-body binding is not sufficient for the two areas to overlap and we cannot obtain a simultaneous description of ^{13}Be and ^{14}Be .

The probabilities of the main components of the three-body wave function, in the jj -coupling scheme, are presented in Fig. 8. We study the β dependence of these probabilities for fixed V_{ls} of -2.5 MeV. We see that the main component in the ground state wave function is $(s_{1/2})^2 \otimes 0^+$, being 45% for $\beta = 0.8$ and $V_{ls} = -2.5$ MeV. The probability associated with this component decreases rapidly with β , whereas the probability of core excited components increases with β , since the coupling with the excited core state is strong. The $(d_{5/2})^2 \otimes 0^+$ probability is small compared to that for $(s_{1/2})^2 \otimes 0^+$ and is only 8.5% for $\beta = 0.8$ and $V_{ls} = -2.5$ MeV. This component is almost constant for large β and changes when $|\beta| \rightarrow 0$. The core excited components are very small for negative β , e.g. for $\beta = -1.0$ and $V_{ls} = -2.5$ MeV the wave function is 70% of $(s_{1/2})^2 \otimes 0^+$, 10% of $(d_{5/2})^2 \otimes 0^+$, 4% of $(d_{3/2})^2 \otimes 0^+$ and the remaining 16% is spread over the many core excited components. For positive β the $(d_{5/2})^2 \otimes 2^+$ and $(s_{1/2}, d_{5/2}) \otimes 2^+$ probabilities increase with β and are 10% each when $\beta = 0.8$ and $V_{ls} = -2.5$ MeV, while the other components are comparatively small.

The β dependence of the summed probabilities of all wave function configurations with an excited core is shown on Fig. 9 for three values of V_{ls} . We note that the probability of the core excited components increases with β , and very quickly for positive deformations. The probability rises from 0.0 % for zero deformation to nearly 45% for $\beta = 1$. For negative β the probability of excited core components rises to a maximum of only 15%. The probabilities do not change significantly with V_{ls} .

The halo in light nuclei is favored if the ground state of the nucleus contains a significant *s*-wave component. We have assumed that the ground state of ^{13}Be is an *s*-state and calculate that the main component of the three-body wave function is also an *s*-state. We find that the ^{14}Be ground state is consistent with a large core deformation and hence contains a large admixture of core excited components, being nearly 40% for $\beta = 0.8$ and $V_{ls} = -2.5$ MeV.

4 Conclusions

In this paper we have obtained a range of three-body model space parameters (V_0, β, V_{ls}) which are able to describe correctly the available experimental data for ^{13}Be and ^{14}Be . These include the Borromean property of the ^{14}Be system, the position of the $5/2^+$ resonance in ^{13}Be , the large quadrupole deformation of ^{12}Be , and the observed two-neutron separation energy of ^{14}Be .

We have assumed that ^{14}Be is represented as a deformed core plus two neutrons, three-cluster system. For simplicity we use a particle-rotor model for ^{13}Be , assuming that the 0^+ and 2^+ states in ^{12}Be form the lowest two members of a $K = 0$ rotational band, and that there are no other relevant low-lying excited states in the core. The resulting three-body problem was solved using the hyperspherical expansion method. The Pauli Principle treatment consisted of projecting the forbidden states out of the space of allowed three-body solutions, assuming that the ^{12}Be core is a closed *p*-shell nucleus.

Assuming standard potential geometry parameters we find that, for large positive quadrupole core deformations, $\beta > 0.8$, depths of the Woods-Saxon and spin-orbit potentials can be found such that the $1/2^+$ ^{13}Be ground state is unbound and ^{14}Be has a two-neutron separation energy of more than 1 MeV. To achieve this we require weak spin-orbit potential strengths, of less than 3 MeV, and comparatively shallow deformed Woods-Saxon potentials. The calculated three-body ^{14}Be ground state wave function has *s*-waves as its main component (45%), reflecting the halo properties of this nucleus. The excited core component in the case that $\beta = 0.8$ and $V_{ls} = -2.5$ MeV is approximately 35%. The implications of this deformed core three-body wave function for the radius of ^{14}Be deduced from interaction cross section measurements will be

discussed elsewhere [36].

5 Acknowledgments

The authors would like to thank Prof. M.V. Zhukov for many useful discussions. The financial support of the University of Surrey and of an Overseas Research Scholarship, for TT, is also gratefully acknowledged. The work was also supported by UK Engineering and Physical Sciences Research Council (EPSRC) Grant number GR/M82141.

References

- [1] R. Gilman *et al.*, Phys. Rev. C **30** (1984) 958
- [2] J.M. Wouters *et al.*, Z. Phys. A **331** (1988) 1
- [3] G. Audi and H.Wapstra, Nucl. Phys. A **565** (1993) 163
- [4] M. Labiche *et al.*, Phys. Rev. Lett. **86** (2001) 600
- [5] D.V. Aleksandrov *et al.*, Sov. J. Nucl. Phys. **37** (1983) 3
- [6] A.N. Ostrowski *et al.*, Z. Phys. A **343** (1992) 489
- [7] A.A. Korshennikov *et al.*, Nucl. Phys. A **588** (1995) 23c
- [8] A.V. Belozyorov *et al.*, Nucl. Phys. A **636** (1998) 419
- [9] A.M. Poskanzer *et al.*, Phys. Rev. Lett. **17** (1966) 1271
- [10] A.G. Artukh *et al.*, Phys. Lett. B **33** (1970) 407
- [11] J.D. Bowman *et al.*, Phys. Rev. Lett. **31** (1973) 614
J.D. Bowman *et al.*, Phys. Rev. C **9** (1974) 836
- [12] M. Thoennessen *et al.*, Phys. Rev. C **63** (2001) 014308
- [13] D.E. Alburger *et al.*, Phys. Rev. C **17** (1978) 1525;
D.E. Alburger *et al.*, Phys. Rev. C **18** (1978) 2727
- [14] H.T. Fortune *et al.*, Phys. Rev. C **50** (1994) 1355
- [15] H. Iwasaki *et al.*, Phys. Lett. B **481** (2000) 7
- [16] A. Navin *et al.*, Phys. Rev. Lett. **85** (2000) 266
- [17] H. Iwasaki *et al.*, Phys. Lett. B **491** (2000) 8
- [18] G.F. Bertsch and H. Esbensen, Ann. Phys. (N.Y.) **209** (1991) 327

- [19] M. Labiche, F.M. Marqués, et al., Phys.Rev C **60** (1999) 027303
- [20] I.J. Thompson and M.V. Zhukov, Phys.Rev C **53** (1996) 708
- [21] P. Descouvemont, Phys.Rev. C **52** (1995) 704
- [22] A. Adahchour *et al.*, Phys. Lett. B **356** (1995) 445
- [23] D. Baye, Nucl. Phys. A **627** (1997) 305
- [24] F.M. Nunes, I.J. Thompson and R.C. Johnson, Nucl.Phys. A **596** (1996) 171
- [25] F.M. Nunes, J.A. Christley, I.J. Thompson, R.C. Johnson and V.D. Efros, Nucl. Phys. A **609** (1996) 43
- [26] F.M. Nunes, I.J. Thompson, J.A. Tostevin, Nucl. Phys. A **703** (2002) 593
- [27] H. Esbensen, B.A. Brown and H. Sagawa, Phys. Rev. C **51** (1995) 1274
- [28] D. Ridikas, M.H. Smedberg, J.S. Vaagen and M.V. Zhukov, Nucl. Phys. A **628** (1998) 363
- [29] D.Gogny, P. Pires and R. Tourriel, Phys. Lett. B **32** (1970) 591
- [30] F. Nunes, Core Excitation in Few Body Systems: Application to halo nuclei, PhD thesis, University of Surrey, October 1995
- [31] D. Baye, M. Hesse, J.-M. Sparenberg and M. Vincke, J.Phys. B: At. Mol. Opt. Phys. **31** (1998) 3439
- [32] H. Feshbach, Ann. Phys. **19** (1962) 287
- [33] S. Saito, Prog. Theor. Phys. **41** (1969) 705
- [34] I.J. Thompson and B.V. Danilin, private communication
- [35] M.V. Zhukov *et al.*, Phys. Rep. **231** (1993) 153
- [36] T.Tarutina, I.J.Thompson, J.A.Tostevin, in preparation

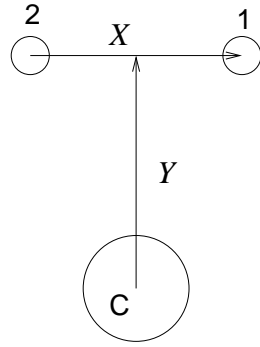


Fig. 1. The \mathbf{T} -set of Jacobi coordinates.

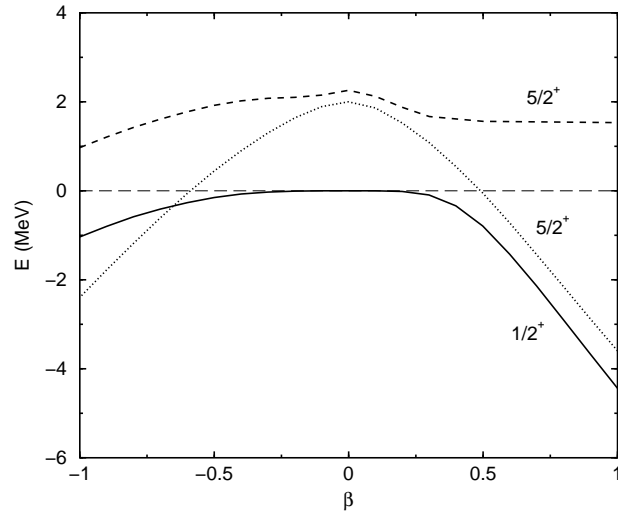


Fig. 2. The deformation dependence of the two $5/2^+$ states and the $1/2^+$ state in ^{13}Be when $V_{ls} = -8$ MeV, and other model parameters are fixed (see text).

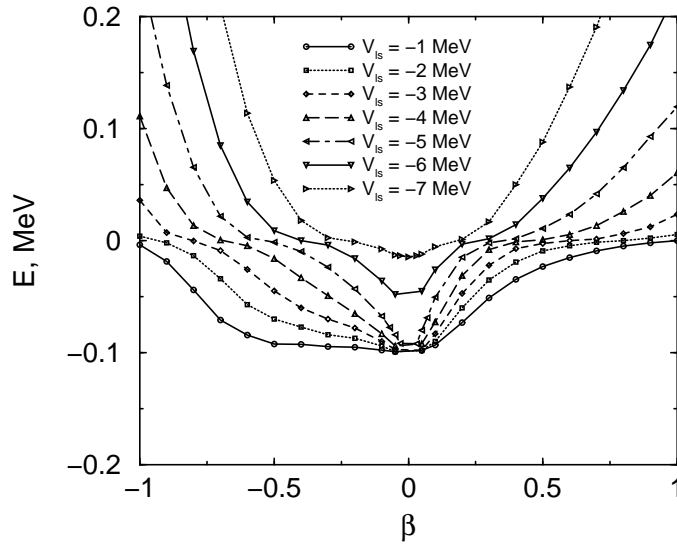


Fig. 3. The deformation dependence of the $1/2^+$ level in ^{13}Be for different values of spin-orbit depth V_{ls} . The central potential strength V_0 was adjusted for each β to keep the lowest $5/2^+$ state at 2 MeV.

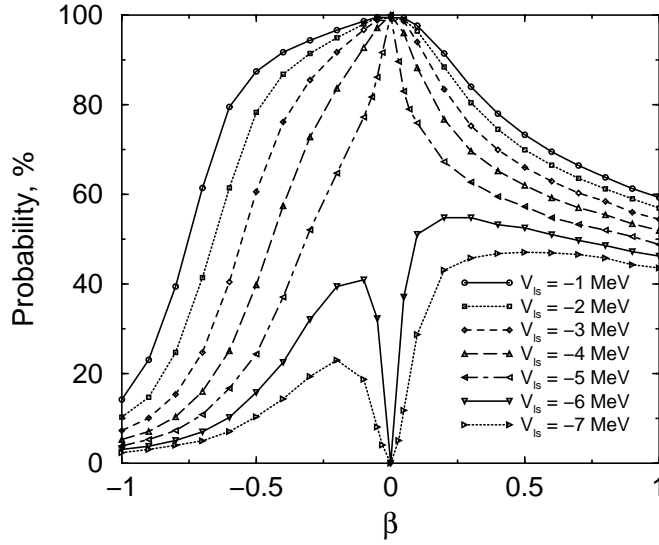


Fig. 4. Percentage of core excited components in the $^{13}\text{Be } 5/2^+$ resonance fixed at 2 MeV by varying V_0 for each β .

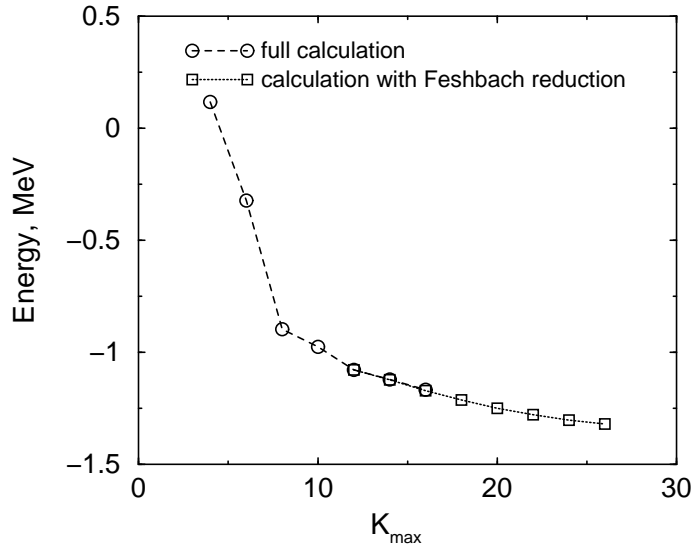


Fig. 5. Convergence of the three-body ground state energy of ^{14}Be , with the maximum number of hyperspherical harmonics K_{max} . The dashed curve and open circles represent full coupled channels calculations. The dotted curve and open squares represent the calculations for each K_{max} , but with the number of hyperspherical harmonics treated exactly reduced to 12.

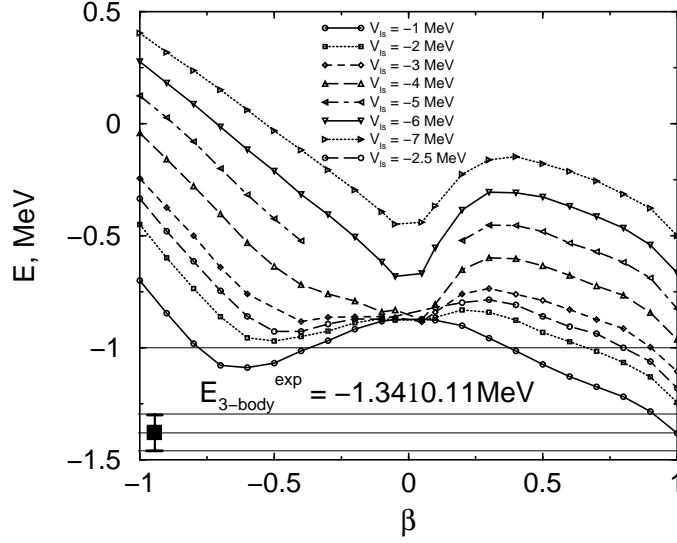


Fig. 6. Deformation dependence of the three-body binding energy of ^{14}Be , calculated using the adjusted Woods-Saxon potential parameters for a set of spin-orbit depths, at each β varying V_0 as in Figs. 3 and 4.

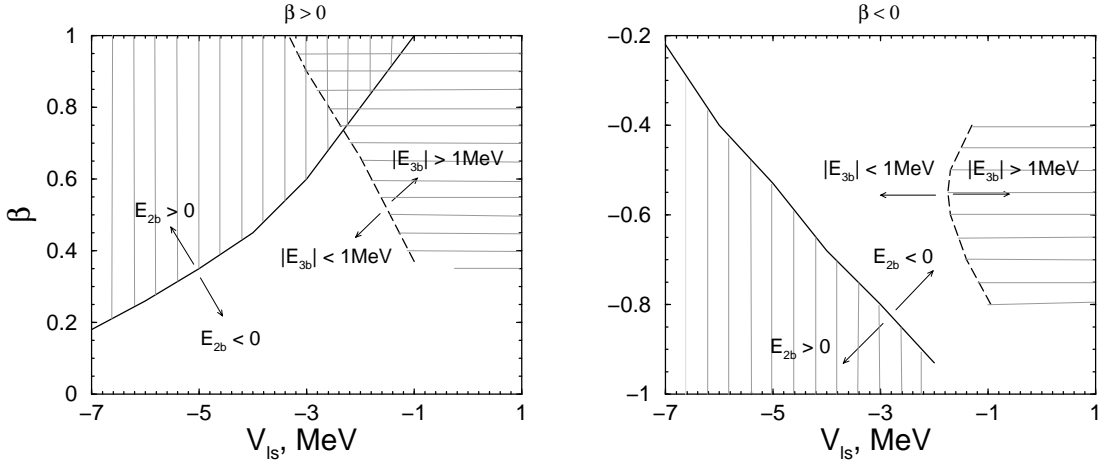


Fig. 7. The region of β and V_{ls} which describes ^{13}Be and ^{14}Be simultaneously. The left panel corresponds to positive β and the right to negative β . The solid lines correspond to the limit of no binding in ^{13}Be ($E_{2b} = 0$), the dashed lines correspond to a two-neutron separation energy in ^{14}Be E_{3b} equal to 1 MeV. The shaded area to the left from the solid line represents the area of parameters where ^{13}Be is unbound and the shaded area to the right from the dashed line shows the area where the binding energy of ^{14}Be is larger than 1 MeV. The overlap of this areas represents the area of parameters where the simultaneous description of ^{13}Be and ^{14}Be is achieved. It is seen that this is possible only for large positive deformations.

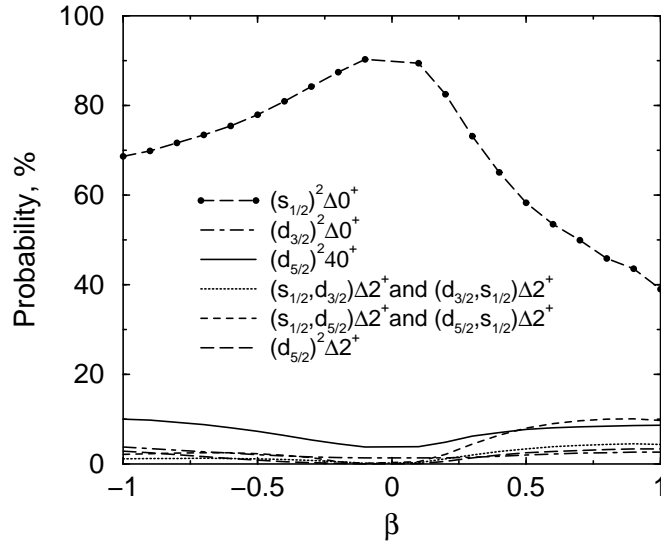


Fig. 8. Probabilities of the main components in the three-body wave function of ^{14}Be as a function of β , for the case with fixed spin-orbit depth $V_{Is} = -2.5$ MeV.

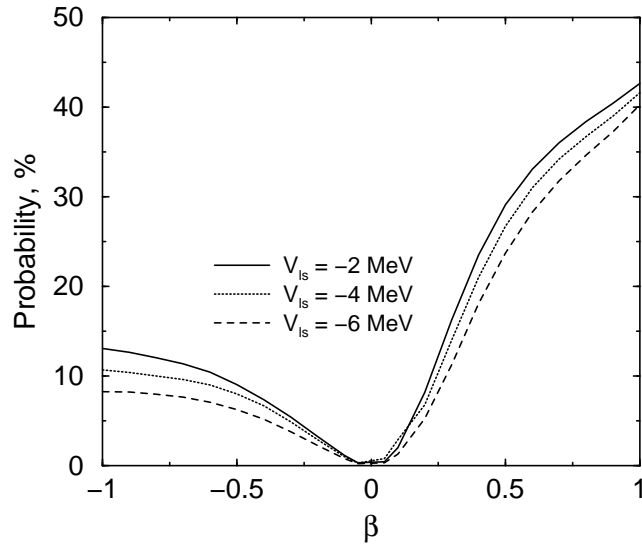


Fig. 9. The total excited core components in the ^{14}Be ground state three-body wave function as a function of core deformation β for several values of V_{Is} .